Russian Journal of Biomechanics, № 1: 75-88, 1999

OBJECT DETECTION IN MEDICAL IMAGES BASED ON IMPROVED MORPHOLOGICAL MULTIRESOLUTION DECOMPOSITION AND MORPHOLOGICAL SEGMENTATION

W. Li, V. Haese-Coat and J. Ronsin

INSA, Laboratoire ARTIST; 20, Avenue des Buttes de Coesmes, 35043 RENNES, FRANCE

Abstract: A semi-automatic object detection method based on mathematical morphology image processing techniques is presented. This paper does not present a complete methodology but rather an illustration of a potential application of mathematical morphology to medical images. The method based on mathematical morphology tools includes an improved multiresolution morphological decomposition algorithm (IMMD) and other morphological segmentation techniques. In IMMD, a group of openings by morphological reconstruction with different structuring elements permits a size-oriented object decomposition. Each image component contains objects with a limited size distribution, and the original image can be completely reconstructed by addition, from these decomposed images. Thus, specific methods can be employed separately on these image components for a better segmentation result. Image processing techniques based on mathematical morphology including morphological filtering, morphological gradient transform, dilation, hit/miss transform and so on, are employed in the segmentation procedures. In applications to object detection of various medical CT (Computer Tomography) and MR (Magnetic Resonance) images, fairly good results have been obtained which show that this approach bears higher degree of segmentation accuracy and consistency.

Key words: mathematical morphology, multiresolution decomposition, image segmentation, object detection

Introduction

The first step in image analysis generally is to segment the image. Segmentation subdivides an image into its constituent parts or objects. Automatic (semi-automatic) segmentation of objects from medical images serves as the key step in applications such as computer aided diagnosis, quantization studies and computer assisted surgery. In many cases, it is quite difficult to extract regions with pathological interests from medical images using general purpose methods, especially when objects (organs, pathological zones) to be detected on image are visually partially mixed with their neighbouring structures.

Generally, a complete image segmentation procedure can be divided into three steps: (1) preprocessing, which includes image simplification, noise filtering, image normalization, etc.; (2) edge detection (for edge-based methods) or feature extraction followed by classification (for region-based methods); (3) postprocessing, which includes all image improvement methods. Concerning to morphological segmentation problem, the general approach involves: image simplification, marker extraction and contour detection [1, 2]. The image simplification removes the useless information, the marker extraction identifies the presence of homogeneous regions and the contour detection locates the edges of the previous extracted regions. In medical image segmentation applications, techniques based on mathematical morphology are beginning to become very important tools. Their recent applications in vascular network segmentation on micrographs and internal structures segmentation on 3D MR images can be found in [3, 4].

After a brief review of mathematical morphology basic principles and tools, this paper proposes a method for semi-automatic detection and segmentation of objects from medical images using mathematical morphology techniques. The method can be considered as an illustration of the last developed morphological tools rather than a complete methodology. In a previous paper [5], we had presented classical morphological techniques applied to medical image fusion. Here, an improved decomposition technique based on the multiresolution morphological decomposition algorithm proposed by Wang et al. [6] is introduced. This technique permits a better size-oriented object decomposition and will be used in the object isolation procedures. In our image segmentation procedures, various techniques based on mathematical morphology [7, 8] are employed for object detection and segmentation. These techniques are incorporated in image filtering, object isolation, edge detection and postprocessings. Applications to object detection and segmentation of CT and MR images illustrate the reliability and efficiency of the proposed method.

In the following parts of the paper, we recall briefly mathematical morphology fundamentals. Then, an improved multiresolution morphological decomposition algorithm is proposed, various object detection techniques based on mathematical morphology are introduced to construct our complete image segmentation diagram, and experimental results are finally given.

Review of Mathematical Morphology [8]

The basic operations of mathematical morphology are erosion, dilation, opening, and closing. We consider a binary image as a set X in N-dimension Euclidean space E^N. Let the compact set $B \in E^N$ denote the structuring element which is usually a set with simple shape. The translation of X by a point $z \in E^N$ is denoted by X_z and is defined by $X_z = \{ x + z \mid x \in X\}$. Then the binary erosion of X by B denoted by $X \ominus B$ (or $\varepsilon_B(X)$) and the binary dilation denoted by $X \oplus B$ (or $\delta_B(X)$) are defined as follows:

$$X \ominus B = \{ z \mid B_z \subseteq X\} = \bigcap_{b \in B} X_{-b},$$

$$X \oplus B = \{ x + b \mid x \in X,\ b \in B\} = \bigcup_{b \in B} X_b.$$

When X has been eroded by B, it is not possible, in general, to recover the initial set X by dilating the eroded set. When relying on this remark, it is possible to define two other operations: opening and closing. The opening of X by B is denoted by $X \circ B$ (or $\gamma_B(X)$) and is defined by:

$$X \circ B = (X \ominus B) \oplus B.$$

Similarly, the closing of X by B, denoted by $X \bullet B$ (or $\varphi_B(X)$), is defined as:

$$X \bullet B = (X \oplus B) \ominus B.$$

Generally, erosion shrinks image objects, whereas, dilation expands them. Opening cuts out the narrow isthmuses, suppresses the islands and the capes smaller than the structuring element used, whereas, closing operation fills in small holes and thin gulfs.

Binary mathematical morphology has been extended to grayscale image by using function umbra to make a connection between sets and functions. Let function $f(x) \in E$ be defined on a subset of N-dimensional Euclidean space E^N. The umbra of $f(x)$ is a (N+1)-dimension set defined as:

$$U(f) = \{(x, a) \mid a \leq f(x)\},$$

i.e., the umbra is the set of points *on* and *below* the surface represented by $f(x)$. The function can be reconstructed from its umbra since

$$f(x) = T[U(f)]\,(x) = max\ \{ a \mid (x, a) \in U(f)\}.$$

Suppose a structuring element is a function $h(x) \in E$ defined on subset B of E^N. Eroding or dilating the umbra of $f(x)$ by the umbra of $h(x)$ yields the umbra of a new function, i.e. the erosion or dilation of $f(x)$ by $h(x)$. These two new functions can be computed from the direct formulae:

$$(f \ominus h)(x) = min\ \{ f(x + z) - h(z) \mid z \in B\}, \quad (1)$$
$$(f \oplus h)(x) = max\ \{ f(x - z) + h(z) \mid z \in B\}. \quad (2)$$

The opening and closing of $f(x)$ by $h(x)$ are defined respectively as:

$$f \circ h = (f \ominus h) \oplus h, \quad (3)$$
$$f \bullet h = (f \oplus h) \ominus h.$$

Alternatively, the opening of $f(x)$ by $h(x)$ can be expressed by :

$$f \circ h = T\left[\bigcup_{U(h)_b \subseteq U(f)} U(h)_b \right]. \quad (4)$$

If the structuring element is a set B in E^N, i.e., $h(x) = 0$, $x \in B$, it is called the *plane structuring element*. In this case, the definitions (1), (2) and (3) are conventionally expressed as

$$(f \ominus B)(x) = min\{ f(x + z) \mid z \in B\}, \quad (5)$$
$$(f \oplus B)(x) = max\{ f(x - z) \mid z \in B\}, \quad (6)$$
$$f \circ B = (f \ominus B) \oplus B. \quad (7)$$

Plane structuring elements are widely used in grayscale mathematical morphology since they demand less computations than non-plane ones.

Improved Multiresolution Morphological Decomposition

This section describes the improved multiresolution morphological decomposition algorithm (IMMD). The traditional MMD algorithm is briefly recalled and its drawback in object decomposition is demonstrated. Then the morphological reconstruction is briefly recalled and employed to implement the IMMD algorithm. The improvement and efficiency using the IMMD in size-oriented object decomposition is well illustrated.

1. The Multiresolution Morphological Decomposition

The multiresolution morphological decomposition (MMD) proposed by Wang et al. is based on the basic granulometric theory [9]. Granulometry aims to separate objects into several classes, according to their size. In MMD, a family of flat structuring elements B_i of different sizes is built by the following relation:

$$B_{i+1} = B_i \oplus B,\ i = 0, 1, ..., n\text{-}1, \quad (8)$$

where $B_0 = \{0, 0\}$ and B is an elementary structuring element in E^2 with a simple and regular form such as square, cross or circle. The opening of an image $f(x, y)$ first by using the largest structuring element B_n gives a corresponding filtered output image $s_0(x,y)$ with $s_0(x,y)=\gamma_{B_n}\{f(x,y)\}$. All objects of the image which are larger than B_n will be kept in $s_0(x,y)$. The objects which are a little smaller than B_n and consequently are eliminated from $s_0(x,y)$, can then be extracted in the residue image $f(x,y)$-$s_0(x,y)$ with the second largest structuring element B_{n-1}. Then, smaller and smaller objects are extracted iteratively by successively smaller structuring elements. Thus MMD can be described mathematically as

$$\begin{cases} f_0(x,y) = f(x,y), \\ s_i(x,y) = \gamma_{B_{n-i}}\{f_i(x,y)\}, \quad i = 0, 1, ..., n, \\ f_{i+1}(x,y) = f_i(x,y) - s_i(x,y). \end{cases} \tag{9}$$

The most important property of MMD is that the original image $f(x,y)$ can be exactly reconstructed by its component images as Euclid said " the whole is equal to the sum of its parts", i.e., $f(x,y) = \sum_{i=0}^{n} s_i(x,y)$.

A drawback of traditional MMD is that the decomposition result depends greatly on the size and shape of the set of structuring elements B_i employed. Each component is obtained, based on the possibility to plug into it, structuring elements of a given size. When an object has a shape close to structuring elements, two cases must be considered. In the first case, the structuring element does not fit into the object. So the object will be examined at the next iteration by smaller structuring element (and will lead to the second case). In the second case, the structuring element fits to the central part of the object and extracts it but leads to fragments in the periphery of the objects which are rejected for examination at the next iteration. Thus, we can not obtain a good size-oriented object decomposition result. An illustration of this drawback can be found in Figures 2(a), 2(b) and 2(c) which are component images of Figure 1 (a texture image "cane" taken from Brodatz texture album [10]) passing by MMD. In openings, square structuring elements of sizes 9×9, 5×5, and 1×1 are used. It can be seen that the component image $s_0(x,y)$ (Fig. 2(a)) corresponding to the structuring element 9×9 contains the image background since all objects in the image are smaller than 9×9. The component image $s_1(x,y)$ (Fig. 2(b)) corresponding to the structuring element 5×5 keeps

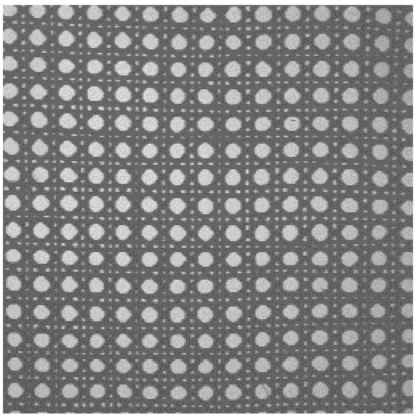

Fig. 1. Texture image used for decomposition.

larger bright round objects of original image, and all rest smaller objects are decomposed into $s_2(x,y)$ (Fig. 2(c)). But it can also be seen from these component images that the shape of the employed structuring elements consequently affects the decomposition result very much. Caused by using the square structuring elements in MMD, all objects in these component images assume more or less square forms. It can be seen further more that all object fragments are rejected at the last iteration (in our case, the component image $s_2(x,y)$) after the successive subtractions between component images, and according to our experiments, the size of fragments on this component image varies depending on the choice of the structuring elements B_i.

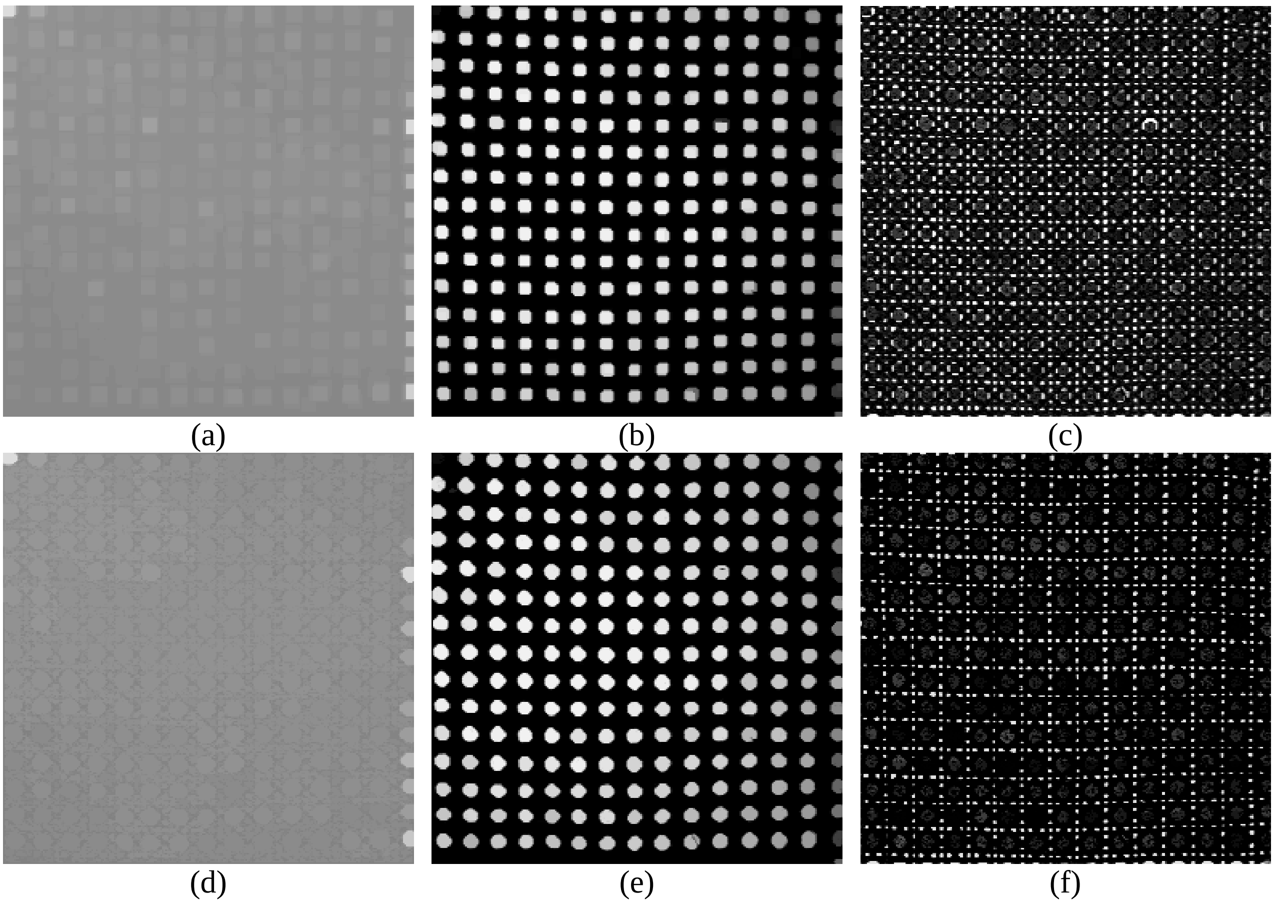

Fig. 2. Texture image of Fig. 1 decomposed by different algorithms. (a~c) shows the decomposition results using MMD; (d~f) shows the decomposition results using IMMD.

In order to separate more efficiently the different sized objects into different component images, the morphological openings in traditional MMD (9) are evidently not suitable, they should be replaced by morphological filters which preserve the connectivity of objects [1]. In the following part, we will introduce the IMMD which is constructed by a connected filter: opening by morphological reconstruction.

2. The Improved Multiresolution Morphological Decomposition

2.1. Filtering by Morphological Reconstruction: Morphological reconstruction operators belong to connected morphological filters. They are based on geodesic transformations [1, 11]. Let *Min* and *Max* denote the pointwise minimum and maximum between two functions and B the flat structuring element, $\delta_B(g)$ ($\varepsilon_B(g)$) is the dilation (erosion) of function g by structuring element B. The elementary geodesic dilation (erosion) of grayscale image g under (over) f is defined as follows:

$$\delta^{(1)}(g, f) = Min\ \{\delta_B(g), f\}, \quad (10)$$

$$\varepsilon^{(1)}(g, f) = Max\ \{\varepsilon_B(g), f\}. \quad (11)$$

Morphological reconstruction by dilation $\gamma^{(rec)}$ (when $g \le f$) and by erosion $\varphi^{(rec)}$ (when $g \ge f$) are iterative operations of elementary geodesic dilation and erosion until idempotence:

$$\gamma^{(rec)}(g, f) = \delta^{(\infty)}(g, f) = \dots\ \delta^{(1)}(\dots\ \delta^{(1)}(g, f)\ \dots, f), \quad (12)$$

$$\varphi^{(rec)}(g, f) = \varepsilon^{(\infty)}(g, f) = \dots\ \varepsilon^{(1)}(\dots\ \varepsilon^{(1)}(g, f)\ \dots, f). \quad (13)$$

In $\gamma^{(rec)}$, g is usually taken as an opening or an erosion of f by a flat structuring element; in $\varphi^{(rec)}$, g is usually taken as a closing or a dilation of f by a flat structuring element.

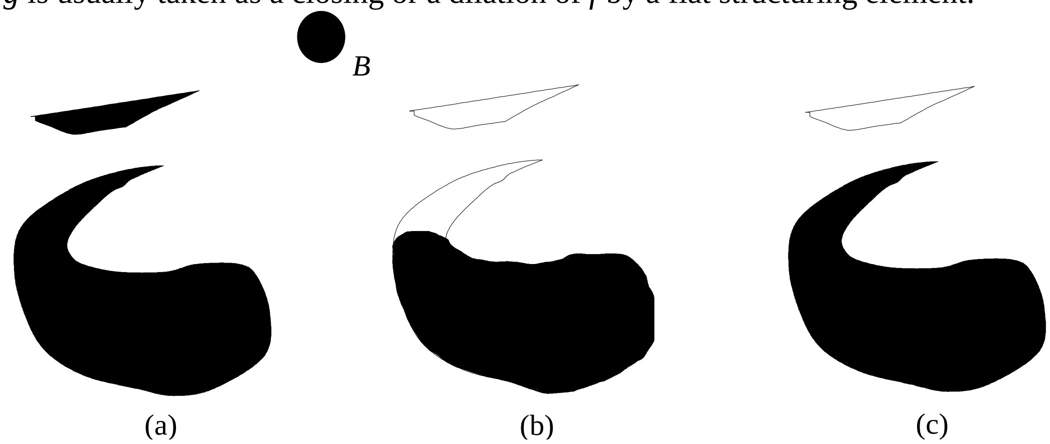

Fig. 3. Results of a binary image (a) which contains two objects with different sizes filtered respectively by the non-connect opening (b) and connected opening (opening by reconstruction) (c) by the same structuring element *B*.

The differences between classical opening and opening by morphological reconstruction on binary images are illustrated in Figure 3. In this example, classical opening and opening by morphological reconstruction are respectively employed on a binary image containing two objects (Fig. 3(a)), the opening breaks one of the two objects (Fig. 3(b)), while the opening by reconstruction preserves well the continuity of this object. Although there exist some differences when morphological reconstruction is applied to graylevel images, it can be proven that filtering by morphological reconstruction has effects of preserving the connectivity, continuity of objects and of removing the useless information on images [1], thus it is more suitable for the size-oriented object detection and extraction problems.

2.2. The Improved Multiresolution Morphological Decomposition: Using opening by morphological reconstruction to replace the opening operation in MMD leads to IMMD as follows:

$$\begin{cases} f_0(x,y) = f(x,y), \\ s_i(x,y) = \gamma^{(rec)}_{Bn-i}\{f_i(x,y)\}, \quad i = 0,1,\dots,n, \\ f_{i+1}(x,y) = f_i(x,y) - s_i(x,y). \end{cases} \quad (14)$$

It can be noticed that equation (14) keeps all properties of equation (9) unchanged.

The advantage of IMMD in object decomposition can be seen in Figures 2(d), 2(e) and 2(f). The decomposition procedures assume exactly the same as in MMD : a texture image (Figure 1) passes by IMMD. In openings by morphological reconstruction, square structuring elements of sizes 9×9, 5×5, and 1×1 are employed. The component images corresponding respectively to the structuring element 9×9, 5×5 and 1×1 are shown in Fig. 2(d), 2(e) and 2(f). It is quite clear that objects in this texture image with different sizes are perfectly separated into different component images, and the decomposition result is rarely affected by the choices of shape and size of structuring elements.

Applications to Object Detection in Medical Images

The IMMD is then employed for region isolation step in object detection applications of medical images. Various mathematical morphology techniques in image processing are used in these medical applications. A semi-automatic object detection scheme is constructed with procedures including preprocessing, region isolation, morphological thinning and postprocessing.

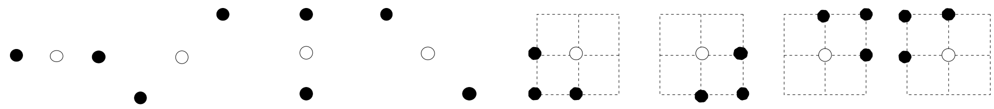

(a) (b)

Fig. 4 : Two series of structuring elements in DMFR. (a) 3-point 4-direction linear structuring element; (b) 4-point 4-direction square structuring element.

1. Preprocessing

Preprocessing aims to simplify medical images, to eliminate the eventual noise and useless information on images and at the same time, to keep image details maximally unchanged. A noise removal and detail preservation scheme using a connected filter, the directional morphological filtering by reconstruction (DMFR) [12], is employed here.

The principle of DMFR is to use a structuring element p of a certain size in several directions u_1, u_2, ..., u_n in morphological opening by reconstruction $\gamma^{(rec)}$ and closing by reconstruction $\varphi^{(rec)}$. Filtering separately in different directions, we search for the maximum (respectively minimum) of openings by reconstruction (respectively closings by reconstruction) and construct the following pairs of algebraic opening γ_p and algebraic closing φ_p:

$$\gamma_p = Max\left\{\gamma^{(rec)}_{(u_1,p)}, \gamma^{(rec)}_{(u_2,p)}, ..., \gamma^{(rec)}_{(u_n,p)}\right\} \quad (15)$$

$$\varphi_p = Min\left\{\varphi^{(rec)}_{(u_1,p)}, \varphi^{(rec)}_{(u_2,p)}, ..., \varphi^{(rec)}_{(u_n,p)}\right\} \quad (16)$$

The cascading of γ_p and φ_p, i.e., $\varphi_p\gamma_p$, constructs a DMFR. It acts better than $\varphi^{(rec)}\gamma^{(rec)}$ and most other smoothing filters. The more directions taken, the more details of images will be preserved.

In considerations of noise removal and detail preserving abilities, two series of useful structuring elements in DMFR (Fig. 4) are proposed.

2. Region Isolation

2.1. Image Decomposition by IMMD: Region isolation is implemented first by the IMMD. To isolate iteratively objects with different sizes from medical images and according to their size distributions, a family of structuring elements B_i which assumes approximately the object size distribution of the processed image is a priori built in IMMD.

2.2. Thresholding the gradient of component image: One or several component images produced by IMMD are chosen according to objects of interest to be segmented. Depending on the needs of radiologists, these component images can be superimposed altogether to form a new image or be considered separately. We construct then a gradient image which is extracted by pointwise maximum of the general morphological gradient (GMG) operation in 4 orientations [13]. If $\varepsilon_1(f)$, $\delta_1(f)$, $\gamma_1(f)$, $\varphi_1(f)$ denote respectively erosion, dilation, opening and closing by an elementary structuring element l, the GMG is described as:

$$g^g = \{g^- + g^+ + (f - \gamma_1(f)) + (\varphi_1(f) - f)\}/2 = \{\delta_1(f) - \varepsilon_1(f) + \varphi_1(f) - \gamma_1(f)\}/2, \qquad (17)$$

where $g^- = f - \varepsilon_1(f)$ (gradient by erosion), $g^+ = \delta_1(f) - f$ (gradient by dilation), $f - \gamma_1(f)$ (Top-Hat transform), $\varphi_1(f) - f$ (anti Top-Hat transform). 3-point linear segment structuring elements with the 4 principal orientations (Fig. 4 (a)) are used to extract possible contours and peaks from different orientations. If $g^g{}_i$ denotes the GMG operator g^g in direction i, our final gradient operation can be expressed as:

$$g^g{}_{max} = Max\{g^g{}_i \mid i=0°, 45°, 90°, 135°\}. \qquad (18)$$

Then a threshold T is used on the gradient image to construct a binary one, we calculate the histogram of the gradient image and take T between 0.9~0.95 of the maximum histogram value. The appropriate value of T has been experimentally determined. A better T should enable the object of interest to be closed at the largest limit.

2.3. Binary dilation: Sometimes a closed object can not be constructed after the thresholding step. To resolve this problem, we can choose a suitable square structuring element and dilate the thresholded binary image. Thus, small gaps can be covered and the object of interest can be well connected before further segmentation.

3. Morphological Thinning

In order to return the connected region to one pixel width from previous processing, a morphological thinning algorithm which is based on the hit/miss transform [7] is applied. Let T be composed of two subsets T^1 and T^2; then the hit/miss transform of X by T is defined as the set of all points where T_x^1 (translate of T^1 by vector x, i.e., $\{x : x\text{-}b\in X\}$) is included in X and T_x^2 is included in X^c (complement of X with respect to $\boldsymbol{Z}^2$). This hit/miss transform denoted by $X\circledast T$ is expressed as:

$$X\circledast T=\{x : T_x^1\subset X;\ T_x^2\subset X^c\}=(X\ominus\breve{T}^1)\cap(X^c\ominus\breve{T}^2), \qquad (19)$$

where $\ominus$ denotes erosion, and $\breve{T}^i$, i=1, 2 denotes the reflection of set T with respect to origin.

$$D^1=\begin{bmatrix}0&0&*\\0&1&1\\ *&1&*\end{bmatrix}\quad D^2=\begin{bmatrix}*&0&0\\1&1&0\\ *&1&*\end{bmatrix}\quad D^3=\begin{bmatrix}*&1&*\\1&1&0\\ *&0&0\end{bmatrix}\quad D^4=\begin{bmatrix}*&1&*\\0&1&1\\0&0&*\end{bmatrix}$$

$$E^1=\begin{bmatrix}0&0&0\\ *&1&*\\1&1&1\end{bmatrix}\quad E^2=\begin{bmatrix}1&*&0\\1&1&0\\1&*&0\end{bmatrix}\quad E^3=\begin{bmatrix}1&1&1\\ *&1&*\\0&0&0\end{bmatrix}\quad E^4=\begin{bmatrix}0&*&1\\0&1&1\\0&*&1\end{bmatrix}$$

Fig. 5. Two groups of templates in morphological thinning algorithm. * denotes "don't care".

Finally, let $X \setminus Y$ be the set difference between X and Y, the thinning of X by T is defined as:

$$X\mathrm{O}T = X \setminus (X{*},\mathrm{O}T), \tag{20}$$

which could be thought of as a search-and-delete process. The operation $X{*},\mathrm{O}T$ locates all occurrences of the template T in X and the operation $\setminus$ removes from X those pixels which are located. To thin X symmetrically, we construct a group of 3×3 templates $\boldsymbol{D}$ and $\boldsymbol{E}$ to remove border points as well as unnecessary points at junctions, with $\boldsymbol{D}=\{D^1, D^2, D^3, D^4\}$, $\boldsymbol{E}=\{E^1, E^2, E^3, E^4\}$ shown in Figure 5. If S represents the previous processed binary image, the first thinning transformation is given by:

$$\Phi\{S, \boldsymbol{D}, \boldsymbol{E}\}=((((((((S\mathrm{O}D^1)\mathrm{O}E^1)\mathrm{O}D^2)\mathrm{O}E^2)\mathrm{O}D^3)\mathrm{O}E^3)\mathrm{O}D^4)\mathrm{O}E^4). \tag{21}$$

The final thinning result can be obtained by repeating this process iteratively until idempotence.

4. Postprocessing

A postprocessing algorithm is constructed to clean automatically the unimportant objects and branches from the thinned image, only the object(s) of interest will be kept in thinned result. This can be done by a simple choice of one point in each closed object on the thinned image, and the contour of the object will be traced automatically by our algorithm. Finally, if we have several objects to detect, we can then superimpose each segmented contour of objects onto the original image to form the final segmented image.

The block diagram of the proposed semi-automatic object detection and segmentation method is illustrated in Figure 6.

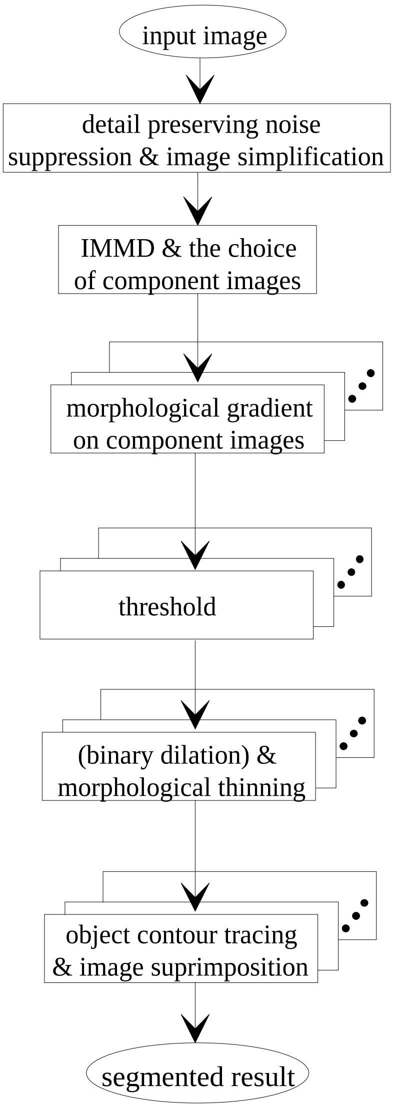

Fig. 6. The block diagram of object detection and segmentation algorithm.

Experimental Results

The proposed object detection and segmentation method is employed on CT and MR medical image segmentation applications. Several spiral CT chest images and MR cerebral images are processed. Two examples are given in the following paragraphs.

1. First Example: Region Segmentation of CT Images

In applications of object detection to spiral CT chest images, our goal is to detect and segment nodule or lesion regions from other organs. These regions in the images are quite difficult to extract by normal edge tracing or thresholding methods because of their eventual tight connection with neighbouring regions. Figure 7(a) shows an example of CT lung image in which a lesion region is situated at the upper left part of lungs, this region is partially connected with neighbouring regions and there is almost no difference in graylevels between this lesion and the muscle regions around. After preprocessing (noise suppression and image simplification by directional morphological filtering by reconstruction), IMMD with a group of square structuring elements of sizes 161×161, 121×121, 81×81, 41×41 and 1×1 is employed to isolate image objects of different sizes. The choice of this set of structuring elements is made to adapt approximately the size distribution of objects of this image.

According to performance, two component images with structuring element sizes 81×81 and 41×41 are evaluated and superimposed to construct a new image (Fig. 7(b)). It can be seen from this new image that the lesion region is well isolated. Fig. 7(c) shows the thresholded image of 7(b) after the morphological gradient operation, the threshold value is 0.95 of the maximum histogram value from the gradient image. To construct a connected lesion region, binary dilation of thresholded image (Fig. 7(c)) with a 7×7 square structuring element is used and the result can be seen on Fig. 7(d). Then morphological thinning algorithm is applied to the dilated image and thinning result is shown on Fig. 7(e). Finally, the thinned image is post processed to eliminate non relevant regions and branches from the lesion region. Fig. 7(f) illustrates the final segmented lesion region superimposed with original image. From other CT images, quite good segmentation results are also obtained.

2. Second Example : Inner Object Segmentation of MR Images

Some applications are equally found in the object detection of MR cerebral images, the aim is to detect and segment tumor regions from normal ones, sometimes we even need to detect the inner objects in a tumor region in order to separate the different internal pathological regions of the tumor. The second example concerns for the inner object detection and segmentation. Figure 8(a) shows a MR cerebral image containing a tumor situated at the central part of the image, some different smaller regions can also be seen from this tumor region. After the preprocessing, IMMD with a group of square structuring elements of sizes 57×57, 43×43, 29×29, 15×15 and 1×1 is executed to isolate image objects of different sizes. The choice of this set of structuring elements is also made to adapt approximately the size distribution of objects of this image. According to the clearance of these component images, the component image corresponding to structuring element 29×29 (Fig. 8(c)) is chosen to segment the global tumor region. Two other inner regions are separated more clearly in the component image with structuring element 15×15 (Fig. 8(d)), and one smaller inner object is isolated in the last component image corresponding to structuring element 1×1. The same segmentation procedures as used in the first example are employed respectively to these three component images. To separate the global tumor region, 0.9 of the maximum histogram value from the gradient image is taken as the threshold value, and no binary dilation is needed, because the contour of this region is closed after thresholding. To process the other two component images, we chose a threshold value equals to 0.95 of the maximum histogram value from the gradient image. To close the contours of the two smaller regions for the image of Fig. 8(d), binary dilation of 3×3 is used. For image of Fig. 8(e), binary dilation is not needed.

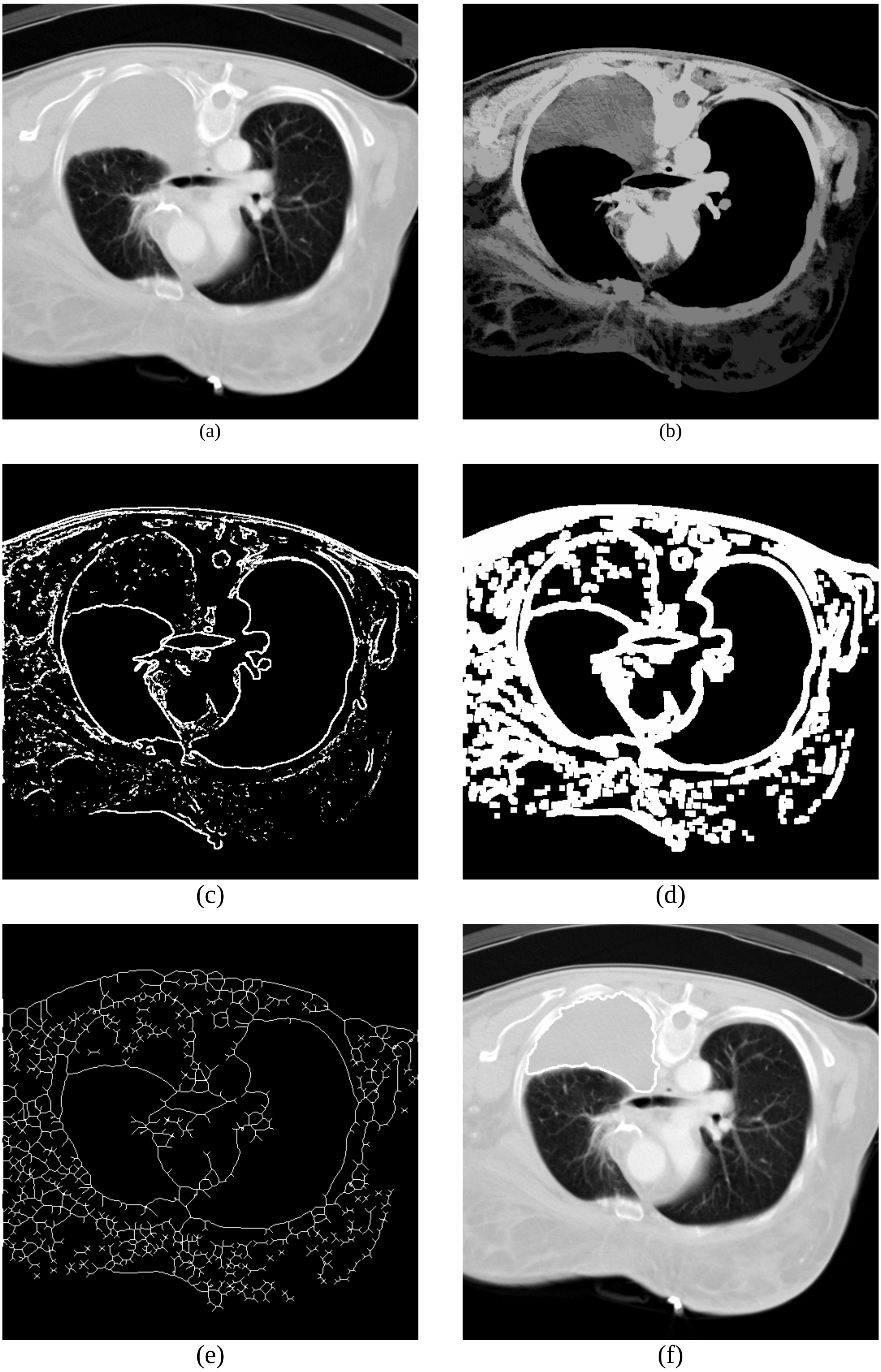

Fig. 7. A spiral CT image (a) and different steps in lesion region segmentation (b), (c), (d) and (e). Final segmentation result is in (f).

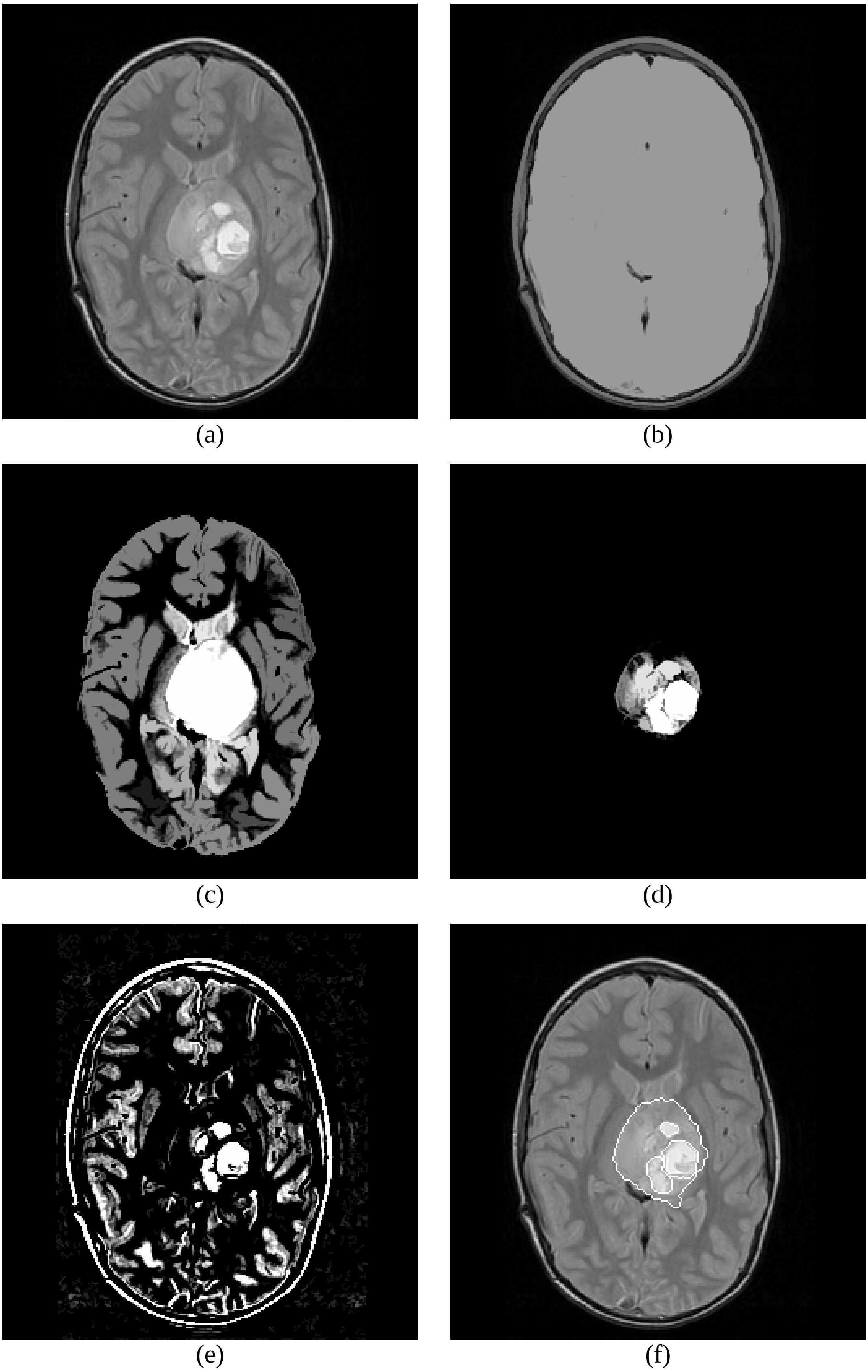

Fig. 8. A MR cerebral image (a) and its different component images which correspond respectively to structuring elements 57×57 (b), 29×29 (c), 15×15 (d) and 1×1 (e) using IMMD. Final segmentation result is illustrated in (f).

Figure 8(f) shows the final segmentation result which is the superimposition of all the three separated results of the component images together onto the original image.

Discussion and Conclusion

This paper illustrates and shows performances of last developments in mathematical morphology image processing techniques when they are applied to medical domain. It is noticeable that the proposed IMMD has advantages in size oriented object detection. Objects with different sizes can be efficiently separated after this decomposition algorithm.

The feasibility of such method has been demonstrated and proven in various applications on CT and MR image segmentations. However, towards an automatic object detection, this method has still some way to go. Actually, the algorithm procedure needs the choice of structuring element sizes and shapes. The choice of shapes is not really critical and can be restricted to square ones in most applications. About structuring element size, the choice simultaneously depends on image resolution and size of objects to segment. In this context, two solutions can be proposed. The first one consists in observing the original image in order to determine the sizes of objects to segment, which define structuring element sizes. The second one can be based on the observation of results obtained by IMMD algorithm using a family of all possible structuring elements and then, selecting those corresponding to components containing the objects to segment.

Obtained results with improved multiresolution morphological decomposition and morphological segmentation show the different advantages of such non linear techniques in medical image segmentation. Indeed, on segmented object, edges are well preserved without any confusion with neighbouring objects on one hand and, object connexity is also kept on the other hand.

Finally, it can be underlined that this segmentation technique is extensible to three-dimensional medical images.

Acknowledgment

The authors would like to thank Dr. Fei Mao, Department of Radiology, University of South Florida, who provided the medical data. His comments were exceptionally useful.

References

1. SALEMBIER P., SERRA J., Flat zones filtering, connected operators, and filters by reconstruction, **IEEE Trans on Image Processing**, 4(8): 1153-1160, 1995.
2. MEYER F., BEUCHER S., Morphological segmentation, **Journal of Visual Communication and Image Representation**, 1(1): 21-46, 1990.
3. THACKRAY B.D., NELSON A.C., Semi-automatic segmentation of vascular network images using a rotating structuring element (ROSE) with mathematical morphology and dual feature thresholding, **IEEE Trans. on Medical Imaging**, 12(3): 385-392, 1993.
4. GERAUD T., MANGIN J.F., BLOCH I., MAITRE H., Segmentation internal structures in 3D MR images of the brain by markovian relaxation on a watershed based adjacency graph, in Proceedings of IEEE International Conference on Image Processing, 3, Washington DC, USA, October, 548-551, 1995.
5. RONSIN J., Mathematical morphology and multiresolution fusion of medical pictures, **Russian Journal of Biomechanics**, 1-2: 61-73, 1997.
6. WANG D., HAESE-COAT V., BRUNO A., RONSIN J., Texture classification and segmentation based on iterative morphological decomposition, **Journal of Visual Communication and Image Representation**, 4(3): 197-214, 1993.
7. SERRA J., **Image Analysis and Mathematical Morphology**, Academic Press, London, 1982.
8. HARALICK R.M., STERNBERG S.R., ZHUANG X., Image analysis using mathematical morphology, **IEEE Trans Pattern Anal Machine Intell**, 9(4): 532-550, 1987.

9. MATHERON G., **Random Sets and Integral Geometry**, Wiley, New York, 1975.
10. BRODATZ P., **Textures**, Dover, New York, 1966.
11. CRESPO J., SERRA J., SCHAFER R., Theoretical aspects of morphological filters by reconstruction, **Signal Processing**, 47: 201-225, 1995.
12. LI W., OGOR B., HAESE-COAT V., RONSIN J., Detail-preserving morphological filters in noise suppression, in Proceedings of International Conference on Signal Processing, Beijing, China, October, 1996.
13. LI W., HAESE-COAT V., RONSIN J., Quantitative evaluation of detail-preserving and noise-removal abilities of morphological filters, in Proceedings of IEEE International Conference on Image Processing, 1, Washington DC, USA, 510-513, October, 1995.

Определение объекта в медицинских изображениях, основанное на улучшенной морфологической многоуровневой декомпозиции и морфологической сегментации

У.Ли, В.Хэз-Коут, Ж.Ронзин (Ренн, Франция)

Получение изображений медицинских объектов играет важную роль в компьютерной диагностике, хирургии и других разделах медицины. Существенным шагом является сегментация изображения для выделения зон, наиболее важных для исследования. Во многих случаях эта операция является весьма сложной.

В данной работе представлен полуавтоматический метод определения объекта, основанный на технике получения изображений с помощью математической морфологии. Данная статья не дает полного изложения методологии, но скорее является иллюстрацией потенциальных возможностей применения математической морфологии для получения изображений в медицине. Представленный метод включает улучшенный алгоритм многоуровневой морфологической декомпозиции и другие алгоритмы морфологической сегментации. В данном методе морфологическая реконструкция с различными структурными элементами позволяет произвести декомпозицию объекта. Каждая компонента изображения содержит объекты с распределением объектов ограниченной величины, и исходное изображение может быть полностью реконструировано путем сложения этих изображений. Следовательно, различные методы могут использоваться отдельно для этих компонент изображения с целью получить лучший результат сегментации. В процедурах сегментации используются различные методы математической морфологии, включая морфологическую фильтрацию, морфологическое градиентное преобразование, дилатацию и т.д. В медицинских приложениях к определению объекта в различных изображениях при компьютерной томографии и магнитном резонансе получены весьма хорошие результаты, что показывает, что данный подход имеет хорошую степень точности и воспроизводимости объекта. Библ. 13.

Ключевые слова: математическая морфология, многоуровневая декомпозиция, сегментация изображений, определение объекта

Received 12 December 1998